Received: June 18, 2015 | Accepted: July 16, 2015 | Web Released: July 25, 2015 CL-150593

Intrinsic Charge Carrier Mobilities at Insulator–Semiconductor Interfaces Probed by Microwave-based Techniques: Studies with Liquid Crystalline Organic Semiconductors

Tsuneaki Sakurai,*[1,2] Yusuke Tsutsui,[1,2] Wookjin Choi,[1,2] and Shu Seki*[1,2]
[1]*Department of Applied Chemistry, Graduate School of Engineering, Osaka University, 2-1 Yamadaoka, Suita, Osaka 565-0871*
[2]*Department of Molecular Engineering, Graduate School of Engineering, Kyoto University, Nishikyo-ku, Kyoto 615-8510*

(E-mail: sakurai-t@moleng.kyoto-u.ac.jp, seki@moleng.kyoto-u.ac.jp)

The intrinsic, local-scale hole and electron mobilities at the interface between perylenediimide (PDI)-based liquid crystalline organic semiconductors and insulating polymers were evaluated by field-induced time-resolved microwave conductivity (FI-TRMC). The PDI liquid crystals having alkyl and semifluoroalkyl tails showed ambipolar hole and electron mobilities of 0.2 and 0.3 $\mathrm{cm^2\,V^{-1}\,s^{-1}}$, respectively. In contrast, the PDI having triethylene glycol and semifluoroalkyl tails showed no significant conductivity, suggesting an important role of side chain structures on the charge transport properties. The FI-TRMC technique demonstrated here serves as a powerful tool to screen out the interfacial structure of liquid crystalline semiconductor materials.

Macroscopic orientation control of liquid crystalline (LC) materials has been of particular interest since its discovery[1] on substrate surfaces, and a variety of "commanding" methods of the orientation have been developed and reported to date.[2] The commanding approach was at first realized by simple rubbing of the substrate surfaces, and subsequently demonstrated by an use of self-assembled monolayer,[3] macromolecules,[4] photoaligned molecular surfaces,[5] and finally by free surfaces.[2] The successful commanding techniques are strongly suggestive of a crucial role of the interface structure between LCs and substrates not only in the macroscopic orientation of the materials but also the short-range order of LCs at the interfaces.

Since the first discovery of discotic LC materials,[6] LC–substrate interactions have become more significant in controlling the orientation because of the relatively weak motivation to produce fundamental 1D columnar structures via π–π stacking interactions in comparison with LCs with covalently extended rod-like mesogens. Moreover, the fundamental π–π stacking interactions preserve the electronic communication among the π-conjugated cores, leading to the semiconducting nature of the LCs materials.[7–9] Considering that many kinds of π-conjugated motifs, designed for the application in organic electronics, have been continuously reported over the recent decades, quick screening of their conductive property is strongly needed. The pulse-radiolysis (PR-) or flash-photolysis (FP-) time-resolved microwave conductivity (TRMC) methods[10,11] have served as a rapid and accurate measurement technique for the screening process because it only requires a small amount of sample and can accept a variety of sample morphologies including crystals, powders, films, and so on. However, in these classical TRMC methods, charge carriers are generated in bulk. Therefore, it is difficult to access the charge carrier transport property at the insulator–semiconductor interfaces.

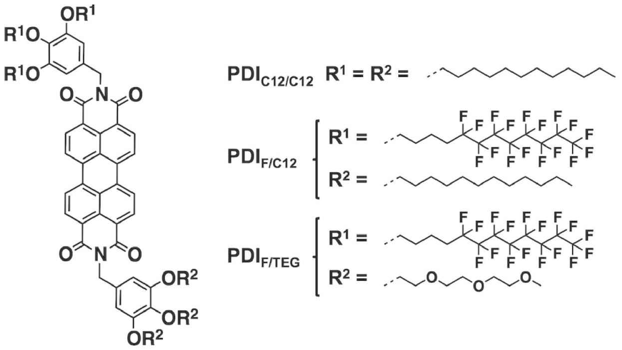

Figure 1. Molecular structures of perylenediimide (PDI) derivatives **PDI$_{\mathbf{C12/C12}}$**, **PDI$_{\mathbf{F/C12}}$**, and **PDI$_{\mathbf{F/TEG}}$**.

To address the interfacial charge carrier mobility, we developed a novel system referred to as field-induced time-resolved microwave conductivity (FI-TRMC).[12–15] In the FI-TRMC technique, simple metal–insulator–semiconductor (MIS) devices are prepared and set into a microwave cavity. Because of the presence of metal electrodes, effective power of the reflected microwave is decreased, giving smaller dynamic range than that of FP-TRMC. However, upon gate bias being applied to MIS devices, we can independently monitor the time dependence of both dielectric loss and injected charge amounts at the interface. These two kinetic traces are overlapped, indicating the accumulated mobile charges solely rely on the observed dielectric loss phenomena. Namely, complete in situ observation is achieved in the FI-TRMC system, leading to the comprehensive analysis of nanometer-scale charge carrier motions at the interface. Furthermore, the polarity of the applied gate bias controls the polarity of the accumulated charge carrier species, enabling the separate evaluation of hole and electron mobilities. In the present work, to confirm the availability of the FI-TRMC technique, we tried to measure spin-coated films of LC semiconductors based on perylenediimide (PDI) derivatives (Figure 1). As a result, we successfully obtained the microwave response as well as charge amount profiles for LC organic semiconductors. Of further interest, obvious effects of side chain structures on the mobility of distinct negative and positive charge carriers as well as density of interfacial carrier traps were clearly demonstrated, proposing the importance of side chains of LC semiconductors on the intrinsic charge carrier transporting phenomena.

PDI-based molecules having immiscible side chain pairs[16,17] were synthesized as described in the Supporting Information. **PDI$_{\mathbf{F/C12}}$** has taper-shaped semifluoroalkyl chains at one imide position while the other imide position carries

Table 1. Phase behaviors with transition temperatures (°C)[a]

Entry	Phase	T / °C (ΔH / kJ mol^{-1})	Phase	T / °C (ΔH / kJ mol^{-1})	Phase	T / °C (ΔH / kJ mol^{-1})	Phase
PDI$_{C12/C12}$	G	−26 (18.1) −31 (−16.3)	Col$_h$	223 (13.7) 220 (−12.3)	IL		
PDI$_{F/C12}$	G	18 (6.2) 10 (−8.2)	Col$_{r1}$	92 (13.4) 114 (3.3) 88 (−17.0)	Col$_{r2}$	240 (15.4) 239 (−21.5)	IL
PDI$_{F/TEG}$	G	56 50	Col$_X$	211 (4.4) 206 (−4.1)	IL		

[a]Transition enthalpies (kJ mol^{-1}) are given in parentheses. Symbols G, Col$_h$, Col$_r$, Col$_X$, and IL denote glassy, hexagonal columnar liquid crystalline, rectangular columnar liquid crystalline, unidentified columnar, and isotropic liquid phases, respectively.

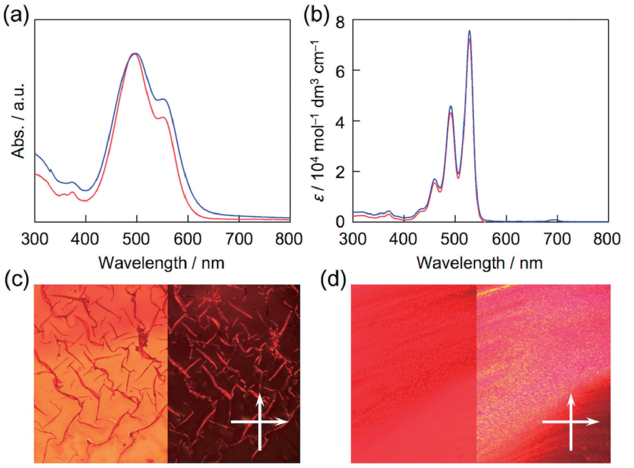

Figure 2. Electronic absorption spectra of **PDI$_{F/C12}$** (red) and **PDI$_{F/TEG}$** (blue) in (a) thin films and (b) CHCl$_3$ solutions at 4×10^{-5} M. Optical (left) and polarized (right) micrographs of spin-coated films of (c) **PDI$_{F/C12}$** and (d) **PDI$_{F/TEG}$**.

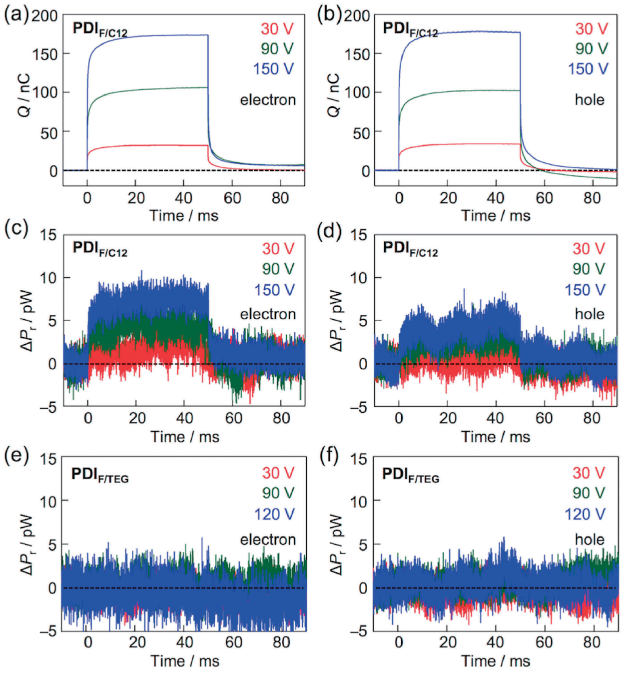

Figure 3. Injected charge amount profiles of **PDI$_{F/C12}$**-based MIS device under applied (a) positive (electron injection) and (b) negative (hole injection) bias. Kinetic traces of changes in reflected microwave power under application of (c) positive and (d) negative bias to **PDI$_{F/C12}$**-based MIS device and (e) positive and (f) negative bias to **PDI$_{F/TEG}$**-based MIS device.

taper-shaped dodecyl chains (Figure 1). **PDI$_{F/TEG}$** is an analogue of **PDI$_{F/C12}$** decorated with semifluoroalkyl/triethylene glycol chains (Figure 1). **PDI$_{C12/C12}$**[18,19] was also synthesized as a reference material exhibiting a typical hexagonal columnar LC phase. A summary of the phase transition profiles is shown in Table 1, where the temperature and enthalpy changes were determined based on differential scanning calorimetry while phase structures were characterized by X-ray diffraction analysis (Figure S1).[20] **PDI$_{F/C12}$** exhibited two rectangular columnar phases with a alkyl/semifluoroalkyl side-chain-segregated packing structure. **PDI$_{F/TEG}$** displayed not a typical LC but a soft crystal. Its mesophase structure of Col$_X$ was unidentified but revealed as a lamellar columnar-based structure. Both PDI molecules form lower-symmetry, structurally higher-ordered assemblies compared to the conventional hexagonal columnar phases. Spin-coated thin films of **PDI$_{F/C12}$** and **PDI$_{F/TEG}$** showed electronic absorption spectra (Figure 2a) characteristic of π-stacked PDI chromophores.[21] In CHCl$_3$ solution, PDI chromophores were molecularly dispersed (Figure 2b). These spectra indicated the side-chain structures essentially did not affect electronic states of PDI moiety. Both spin-coated films showed polydomain textures in optical microscopy and birefringent textures appeared under the crossed polarized condition (Figures 2c and 2d), which indicates that LC columns mostly align parallel to the substrate in the as-cast thin films.

We performed the FI-TRMC technique to evaluate the local-scale charge carrier mobility at insulator/semiconductor interfaces. Analogous to the previous report, a poly(methyl methacrylate) (PMMA) thin film, selected as an insulating polymer, was fabricated by spin-coating onto a SiO$_2$-Au-quartz substrate from a toluene solution.[12–15] Then the semiconducting LCs were spin-coated on the substrate from a THF solution, followed by the deposition of a Au electrode. When the MIS device (Au-SiO$_2$-PMMA-**PDI$_{F/C12}$**-Au) was set in the cavity and subjected to positive gate bias voltages, electrons were injected into the interface between **PDI$_{F/C12}$** and PMMA (Figure 3a). Accordingly, we observed the response of the reflected microwave changes (Figure 3c), indicating that the injected electrons contribute to the local-scale conductivity at the interface. By using the empirical equation between ΔP_r and $\Delta N\mu$,[13] we evaluated the local-scale electron mobility (μ_e) of 0.3 cm^2 V^{-1} s^{-1} from the ΔN–$\Delta N\mu$ plot (Figure 4a). A similar process was carried out for the negative bias condition (Figures 3b and 3d), affording the estimated hole mobility (μ_h) of 0.2 cm^2 V^{-1} s^{-1} for **PDI$_{F/C12}$** (Figure 4a). Meanwhile, the obtained μ_e and μ_h values of **PDI$_{C12/C12}$** were 0.1 and 0.2 cm^2 V^{-1} s^{-1} (Figures 4b, S2, and S3). The evaluated mobilities were larger for **PDI$_{F/C12}$**, which might be correlated with the higher structural ordering in its mesophase at room temperature. The slope of both electron and hole signals in Figures 4a and 4b shows a clear single intersect at $\Delta N = 0$. The intersection of the ΔN–$\Delta N\mu$ plot has been

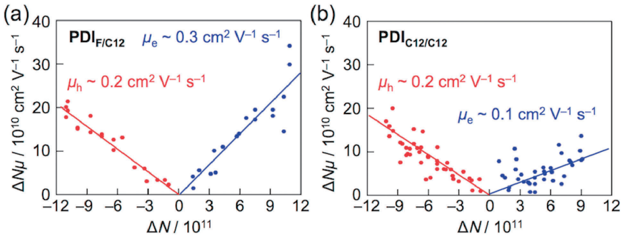

Figure 4. Correlation between the value of ΔN and $\Delta N\mu$, derived independently from the current flow accumulation and microwave dielectric loss measurements, respectively. The value of ΔN was modulated by the bias applied in the range of 0–±150, and an identical MIS device structure was used for (a) **PDI$_{\mathbf{F/C12}}$** and (b) **PDI$_{\mathbf{C12/C12}}$**, respectively. All the measurements were performed at room temperature.

unveiled to give an estimate of defect (trap) density at the interfaces for the injected charge carriers.[14] It should be noted that the trap sites on the substrate was well passivated by the columnar LC molecules in the present system, and no significant contribution from deep traps for charge carriers.

The FI-TRMC profiles of **PDI$_{\mathbf{F/TEG}}$** were totally different from those of the above two compounds. As shown in Figures 3e and 3f, dielectric loss of the microwave was negligible completely upon applied bias voltage of up to ±120 V, where holes and electrons were certainly injected into the device with the clear current flow traces as much as the $3 \times 10^{12}\,\mathrm{cm}^{-2}$ (Figure S4). This is suggestive that the both positive and negative charge carriers accumulated at **PDI$_{\mathbf{F/TEG}}$**–PMMA interfaces are immobilized in glassy solid state of the molecules and/or highly polar TEG chains,[22] even in the present measurement of local scale charge carrier mobility.

The spatial size (Δx) of statistical local motion of charge carriers is estimated during turn-over period of electric field of the probing 9 GHz microwave by the following Kubo equation derived from Einstein–Smoluchowski relation,[23,24]

$$\Delta x = (\mu k_\mathrm{B} T f^{-1} e^{-1})^{1/2} \qquad (1)$$

where k_B, f, and e are Boltzmann's constant, frequency of microwave, and elementary charge, respectively. Provided $\mu = 0.1$–$0.3\,\mathrm{cm}^2\,\mathrm{V}^{-1}\,\mathrm{s}^{-1}$, the value of Δx is given as ca. 5–9 nm. Therefore, charge carrier mobilities with the ambipolar nature derived from FI-TRMC measurement for **PDI$_{\mathbf{C12/C12}}$** and **PDI$_{\mathbf{F/C12}}$**, are suggestive of the delocalization of electron and holes lower than ca. 20 molecules of PDI motifs. The degree of delocalization of charge carriers depends slightly on the columnar stacking fashion (Col$_\mathrm{h}$ and Col$_\mathrm{r}$ in **PDI$_{\mathbf{C12/C12}}$** and **PDI$_{\mathbf{F/C12}}$**, respectively), and more importantly the ambipolar nature of the materials is switched from hole-dominant to electron-dominant ones. The major carrier species along PDI stacks was predicted to depend strongly on the coaxial stacking structures with lateral angles and change from negative (electrons) to positive (holes),[25] and this would be the case giving the switching behavior of the charge carriers observed by FI-TRMC (TRMC@*Interfaces*). Although unique and unclear stacking structures of PDI motifs are still plausible at the interfaces, the switching of the charge carrier species was demonstrated with liquid crystalline PDI motifs in the present study with the non-contact non-destructive probing of charge carrier motion with microwaves, TRMC@*Interfaces*.

This work was partly supported by a Grant-in-Aid for Scientific Research (Nos. 26620104 and 26102001) from the Japan Society for the Promotion of Science (JSPS) and partially supported by Shorai Foundation for Science and Technology.

Supporting Information is available electronically on J-STAGE.

References

1 C. Mauguin, *Bull. Soc. Fr. Mineral.* **1911**, *34*, 71.
2 K. Fukuhara, S. Nagano, M. Hara, T. Seki, *Nat. Commun.* **2014**, *5*, 3320.
3 B. Lee, N. A. Clark, *Science* **2001**, *291*, 2576.
4 T. Kajitani, Y. Suna, A. Kosaka, T. Osawa, S. Fujikawa, M. Takata, T. Fukushima, T. Aida, *J. Am. Chem. Soc.* **2013**, *135*, 14564.
5 K. Ichimura, Y. Suzuki, T. Seki, A. Hosoki, K. Aoki, *Langmuir* **1988**, *4*, 1214.
6 S. Chandrasekhar, B. K. Sadashiva, K. A. Suresh, *Pramana* **1977**, *9*, 471.
7 S. Laschat, A. Baro, N. Steinke, F. Giesselmann, C. Hägele, G. Scalia, R. Judele, E. Kapatsina, S. Sauer, A. Schreivogel, M. Tosoni, *Angew. Chem., Int. Ed.* **2007**, *46*, 4832.
8 J. Hanna, A. Ohno, H. Iino, *Thin Solid Films* **2014**, *554*, 58.
9 M. Funahashi, *J. Mater. Chem. C* **2014**, *2*, 7451.
10 J. M. Warman, A. M. Van De Craats, *Mol. Cryst. Liq. Cryst.* **2003**, *396*, 41.
11 S. Seki, A. Saeki, T. Sakurai, D. Sakamaki, *Phys. Chem. Chem. Phys.* **2014**, *16*, 11093.
12 Y. Honsho, T. Miyakai, T. Sakurai, A. Saeki, S. Seki, *Sci. Rep.* **2013**, *3*, 3182.
13 W. Choi, T. Miyakai, T. Sakurai, A. Saeki, M. Yokoyama, S. Seki, *Appl. Phys. Lett.* **2014**, *105*, 033302.
14 R. Sekiya, Y. Tsutsui, W. Choi, T. Sakurai, S. Seki, Y. Bando, H. Maeda, *Chem. Commun.* **2014**, *50*, 10615.
15 Y. Tsutsui, T. Sakurai, S. Minami, K. Hirano, T. Satoh, W. Matsuda, K. Kato, M. Takata, M. Miura, S. Seki, *Phys. Chem. Chem. Phys.* **2015**, *17*, 9624.
16 T. Sakurai, K. Shi, H. Sato, K. Tashiro, A. Osuka, A. Saeki, S. Seki, S. Tagawa, S. Sasaki, H. Masunaga, K. Osaka, M. Takata, T. Aida, *J. Am. Chem. Soc.* **2008**, *130*, 13812.
17 S. Yagai, S. Okamura, Y. Nakano, M. Yamauchi, K. Kishikawa, T. Karatsu, A. Kitamura, A. Ueno, D. Kuzuhara, H. Yamada, T. Seki, H. Ito, *Nat. Commun.* **2014**, *5*, 4013.
18 Z. An, J. Yu, S. C. Jones, S. Barlow, S. Yoo, B. Domercq, P. Prins, L. D. A. Siebbeles, B. Kippelen, S. R. Marder, *Adv. Mater.* **2005**, *17*, 2580.
19 V. Percec, H.-J. Sun, P. Leowanawat, M. Peterca, R. Graf, H. W. Spiess, X. Zeng, G. Ungar, P. A. Heiney, *J. Am. Chem. Soc.* **2013**, *135*, 4129.
20 Y. Tsutsui, T. Sakurai, K. Kato, M. Takata, S. Seki, *J. Photopolym. Sci. Technol.* **2015**, *28*, 583.
21 S. Ghosh, X.-Q. Li, V. Stepanenko, F. Würthner, *Chem.—Eur. J.* **2008**, *14*, 11343.
22 A. F. Stassen, R. W. I. de Boer, N. N. Iosad, A. F. Morpurgo, *Appl. Phys. Lett.* **2004**, *85*, 3899.
23 R. Kubo, *Rep. Prog. Phys.* **1966**, *29*, 255.
24 R. Kubo, *J. Phys. Soc. Jpn.* **1957**, *12*, 570.
25 V. Marcon, D. W. Breiby, W. Pisula, J. Dahl, J. Kirkpatrick, S. Patwardhan, F. Grozema, D. Andrienko, *J. Am. Chem. Soc.* **2009**, *131*, 11426.